Received: 7 November 2023 | Revised: 7 February 2024 | Accepted: 1 March 2024

DOI: 10.1111/cas.16150

Cancer Science WILEY

ORIGINAL ARTICLE

Long noncoding RNA *TUG1* promotes cisplatin resistance in ovarian cancer via upregulation of DNA polymerase eta

Ryosuke Sonobe[1] | Peng Yang[1,2,3] | Miho M. Suzuki[1] | Keiko Shinjo[1] | Kenta Iijima[1] | Nobuhiro Nishiyama[4,5] | Kanjiro Miyata[6] | Kazunori Kataoka[5] | Hiroaki Kajiyama[2] | Yutaka Kondo[1,7,8]

[1]Division of Cancer Biology, Nagoya University Graduate School of Medicine, Nagoya, Aichi, Japan

[2]Department of Obstetrics and Gynecology, Nagoya University Graduate School of Medicine, Nagoya, Aichi, Japan

[3]Fourth Department of Gynecologic Oncology, Hunan Cancer Hospital/The Affiliated Cancer Hospital of Xiangya School of Medicine, Central South University, Changsha, Hunan, China

[4]Department of Life Science and Technology, School of Life Science and Technology, Tokyo Institute of Technology, Yokohama, Kanagawa, Japan

[5]Innovation Center of Nanomedicine (iCONM), Kawasaki Institute of Industrial Promotion, Kawasaki, Kanagawa, Japan

[6]Department of Materials Engineering, Graduate School of Engineering, The University of Tokyo, Tokyo, Japan

[7]Institute for Glyco-core Research (iGCORE), Nagoya University, Nagoya, Aichi, Japan

[8]Center for One Medicine Innovative Translational Research (COMIT), Nagoya University, Nagoya, Aichi, Japan

Correspondence
Yutaka Kondo, Division of Cancer Biology, Nagoya University Graduate School of Medicine, 65 Tsurumai-cho, Showa-ku, Nagoya, Aichi 466-8550, Japan.
Email: ykondo@med.nagoya-u.ac.jp

Funding information
Japan Agency for Medical Research and Development, Grant/Award Number: 23ama221204h and 23ck0106816h; Japan Society for the Promotion of Science, Grant/Award Number: 23H02747

Abstract

Chemoresistance is a major cause of high mortality and poor survival in patients with ovarian cancer (OVCA). Understanding the mechanisms of chemoresistance is urgently required to develop effective therapeutic approaches to OVCA. Here, we show that expression of the long noncoding RNA, taurine upregulated gene 1 (TUG1), is markedly upregulated in samples from OVCA patients who developed resistance to primary platinum-based therapy. Depletion of TUG1 increased sensitivity to cisplatin in the OVCA cell lines, SKOV3 and KURAMOCHI. Combination therapy of cisplatin with antisense oligonucleotides targeting TUG1 coupled with a drug delivery system effectively relieved the tumor burden in xenograft mouse models. Mechanistically, TUG1 acts as a competing endogenous RNA by downregulating miR-4687-3p and miR-6088, both of which target DNA polymerase eta (POLH), an enzyme required for translesion DNA synthesis. Overexpression of POLH reversed the effect of TUG1 depletion on cisplatin-induced cytotoxicity. Our data suggest that TUG1 upregulation allows OVCA to tolerate DNA damage via upregulation of POLH; this provides a strong rationale for targeting TUG1 to overcome cisplatin resistance in OVCA.

KEYWORDS
cisplatin, long noncoding RNA, ovarian cancer, POLH, TUG1

Ryosuke Sonobe and Peng Yang contributed equally to the work.

1 | INTRODUCTION

Ovarian cancer (OVCA) is the leading cause of cancer death and the most lethal gynecologic cancer.[1] Due to the absence of specific symptoms and a lack of efficient methods to detect early-stage disease, more than 80% of patients are diagnosed at an advanced stage (International Federation of Gynecology and Obstetrics [FIGO] stages III and IV), resulting in poor survival outcomes.[2] The standard of care for OVCA consists of debulking surgery followed by platinum-based chemotherapy (mainly cisplatin and carboplatin); this treatment has not changed over the last three decades. Approximately 25% of OVCA patients are resistant to platinum-based chemotherapies at the initial chemotherapy.[3] Furthermore, half of the patients who are initially sensitive to platinum-based chemotherapies will suffer recurrence and peritoneal metastases, eventually leading to low overall survival.[4–7] Thus, the limited efficacy of cisplatin-based chemotherapy in OVCA patients is a major problem for OVCA treatment.

Cisplatin-based drugs form DNA adducts that cause DNA interstrand and intrastrand cross-links, leading to genotoxic damage.[8,9] The cisplatin-induced DNA cross-links block transcription and DNA synthesis, resulting in cell cycle arrest. Although cisplatin–DNA adducts are recognized as DNA damage and can be repaired in cells, excessive cisplatin-induced DNA damage induces apoptosis.[9] In OVCA cells, however, there is a high frequency of chemoresistance via multiple mechanisms, such as increased activity of DNA damage repair systems, altered drug transport and metabolism, promotion of the epithelial-to-mesenchymal transition, or altered autophagy.[10,11] Given that the primary target of cisplatin is DNA, the effectiveness of DNA damage repair is one of the most dominant resistance mechanisms.[12] Preclinical evidence shows a strong association between the dysregulation of specific DNA repair pathways and resistance to platinum drugs.[13–16]

Long noncoding RNAs (lncRNAs) regulate many cancer-related genes and are associated with oncogenesis and malignancy.[17,18] Aberrant expression of some lncRNAs has also been implicated in cancer drug resistance.[10,19] Therefore, targeting lncRNAs may represent a novel therapeutic anticancer strategy. Taurine upregulated gene 1 (TUG1) is an oncogenic lncRNA that promotes the progression of various cancers.[20,21] We previously reported that depletion of TUG1 reduces the growth of pancreatic cancer cells in vitro and in vivo.[22] We also demonstrated that TUG1-dependent chemoresistance in pancreatic cancer requires the upregulation of dihydropyrimidine dehydrogenase, which degrades 5-fluorouracil, the standard chemotherapy for pancreatic cancer.[22] TUG1 promotes OVCA cell proliferation, migration, invasion, and metastasis.[23,24] In addition, TUG1-dependent targeting of a microRNA (miRNA), miR-29b-3p, induces autophagy and engenders paclitaxel resistance in OVCA.[25] However, it remains unclear whether TUG1 regulates cisplatin sensitivity in OVCA.

In this study, we found that TUG1 promotes cisplatin resistance in OVCA by upregulating DNA polymerase eta (POLH), which enhances DNA damage tolerance through mediating translesion DNA synthesis (TLS).[26–28] Cisplatin treatment combined with TUG1 depletion effectively inhibited tumor growth in xenograft mouse models, underscoring the efficacy of TUG1 depletion in vivo. Our data provide a strong rationale for targeting TUG1 as a novel therapeutic approach to overcome cisplatin resistance in OVCA.

2 | METHODS

2.1 | Clinical samples

Ovarian cancer ($n=20$) samples were obtained from patients who underwent surgical resection and cisplatin-based chemotherapy at Obstetrics and Gynecology, Nagoya University Hospital. All cases were pathologically diagnosed and had complete clinical information (Table S1). Patients with OVCA were divided into two groups according to disease-free survival (DFS) following surgery: a cisplatin-sensitive group (>200 days, $n=11$) and -resistant group (≤200 days, $n=9$). DFS was defined as the time from chemotherapy initiation to recurrence.

2.2 | RNA-FISH

Ovarian cancer tissues ($n=20$) were fixed for 48 hours in 10% buffered formalin, paraffin embedded, and cut into 5-μm sections.

FIGURE 1 High expression of taurine upregulated gene 1 (TUG1) is associated with cisplatin resistance in ovarian cancer (OVCA) cells. (A) Representative smFISH images of TUG1 (in red) in both cisplatin-sensitive and -resistant OVCA samples. Nuclei are counterstained with DAPI (in blue). Insets in the left panels are magnified in the right panels. Insets in the top panels are further magnified in the bottom panels. (B) Quantification of smFISH experiments in cisplatin-sensitive ($n=11$) and -resistant ($n=9$) OVCA samples. The *y*-axis represents the relative number of TUG1 spots in the nucleus and cytoplasm, normalized to the median in cisplatin-sensitive samples. Data are presented as mean ± SEM. Over 100 cells were analyzed per sample. ns, $p>0.05$; $^{**}p<0.01$; $^{***}p<0.001$, two-sided *t*-test. (C) Kaplan–Meier survival curve for OVCA patients based on TUG1 expression. High group (*Z*-score of TUG1 expression ≥0, $n=69$); low group (*Z*-score of TUG1 expression <0, $n=73$), sourced from the TCGA database. (D) RT-qPCR analysis of TUG1 expression in 12 OVCA cell lines. TUG1 expression is normalized to GAPDH and presented as mean ± SEM, $n=3$. (E) Dose–response curve of cisplatin in ES2, SKOV3, and KURAMOCHI cells transfected with CTRL-ASO, TUG1-ASO#1, or TUG1-ASO#2. The IC50 value for each treatment is indicated in the bottom table. Data are presented as mean ± SEM, $n=3$. (F) TUG1 knockdown efficiency was evaluated by RT-qPCR in ES2, SKOV3, and KURAMOCHI cells 24 h post transfection with CTRL-ASO, TUG1-ASO#1, and TUG1-ASO#2. TUG1 expression is normalized to GAPDH and presented as mean ± SEM, $n=3$. $^{***}p<0.001$, two-sided *t*-test. (G) Dose–response curve of cisplatin in ES2 cells transfected with either vector control or pPGK-TUG1. The IC50 value for each treatment is indicated in the right table. Data are presented as mean ± SEM, $n=3$. (H) Combination indices (CI) for SKOV3 and KURAMOCHI cells under the indicated treatment conditions.

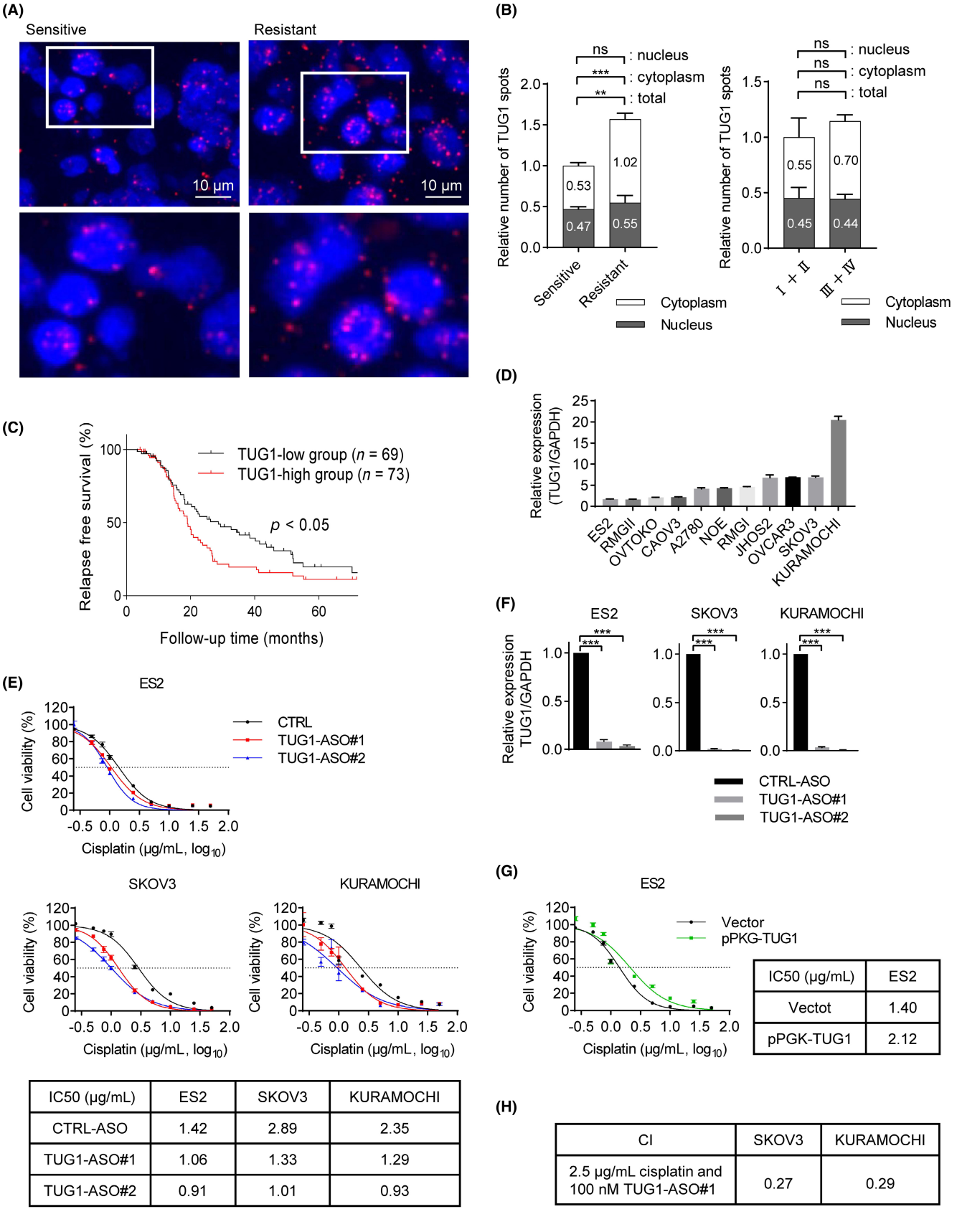

IC50 (μg/mL)	ES2	SKOV3	KURAMOCHI
CTRL-ASO	1.42	2.89	2.35
TUG1-ASO#1	1.06	1.33	1.29
TUG1-ASO#2	0.91	1.01	0.93

IC50 (μg/mL)	ES2
Vectot	1.40
pPGK-TUG1	2.12

(H)

CI	SKOV3	KURAMOCHI
2.5 μg/mL cisplatin and 100 nM TUG1-ASO#1	0.27	0.29

RNA-FISH utilized the ViewRNA ISH Tissue Assay Kit (Thermo Fisher Scientific) and ViewRNA probe set for TUG1 (#VA1-11879, Thermo Fisher Scientific) per the manufacturer's guidelines. Images were captured with a Leica DMI6000 B microscope. TUG1 spots were quantified in ImageJ, with DAPI-stained nuclei as references, counting over 100 cells per sample.

2.3 | TCGA data analysis

TCGA ovarian tumor data were obtained from the GDC Data Portal (https://portal.gdc.cancer.gov), comprising 142 samples with recorded RNA-seq and patient outcomes. Kaplan–Meier DFS curves were created based on TUG1 expression (TUG1-high group, i-score>0, $n=73$; TUG1-low group, Z-score<0, $n=69$) for OVCA patients, with Z-score normalization applied to TUG1 expression in transcripts per million (TPM). TCGA data for miR-4687-3p expression (294 samples) and miR-6088 expression (107 samples) were also sourced from the GDC Data Portal and UCSC Xena (https://xena.ucsc.edu), respectively. Additional details about the analyzed TCGA cases can be found in Table S2.

2.4 | Cell culture

ES2 (ATCC), SKOV3 (RIKEN Cell Bank), KURAMOCHI (JCRB Cell Bank), and SKOV3-Luc (JCRB Cell Bank) cell lines were cultured in RPMI-1640 medium with 10% fetal bovine serum and 1× antibiotic-antimycotic (Anti-anti, Gibco, Thermo Fisher Scientific). All lines were analyzed within 6 months post thawing, authenticated by JCRB Cell Bank via short tandem repeat profiling, and confirmed mycoplasma-free upon thawing. Characteristics of these cell lines are detailed in Table S3

2.5 | Cell transfections

Gene knockdowns and plasmid transfections were carried out with Lipofectamine 3000 (Thermo Fisher Scientific) or ScreenFect A Plus (FUJIFILM Wako Pure Chemical) according to the manufacturer's instructions. Cells were transfected with 100 nM antisense oligonucleotide (ASO), 50 nM miRNA inhibitor, or 50 nM miRNA mimic. A list of ASOs, plasmids, miRNA inhibitors, and miRNA mimics is provided in Table S6.

2.6 | RT-qPCR

RNA extraction and RT-qPCR for *TUG1* and *POLH* was performed as described previously.[18] miRNA RT-qPCR was conducted according to Balcells et al.[29] Target gene expression levels were quantified using GAPDH or RNU6b as internal controls. Oligonucleotide primer details are in Table S6.

2.7 | Drug sensitivity assay

Cells transfected with 100 nM ASO for 24 h in six wells were trypsinized and seeded onto 96-well plates at 1×10^4 cells/well followed by cisplatin treatment (P4394, Sigma Aldrich) for another 48 h. Cell viability was assessed using Cell Count Reagent SF (Nacalai Tesque). The assay was conducted in triplicate. Drug sensitivity was determined by the half-maximal inhibitory concentration (IC50) value using GraphPad Prism8 (GraphPad Software).

2.8 | Global expression analysis of miRNA

miRNA microarrays were processed as described previously,[20] scanned using an Agilent Microarray Scanner (G2565BA, Agilent Technologies), and analyzed using the Feature Extraction software, version 12.0 (Agilent Technologies) with background correction. Data analyses were performed with GeneSpring GX, version 7.3.1 (Agilent Technologies). Expression data were centered on a median using the GeneSpring normalization option. Experiments were performed in duplicate throughout the analysis.

2.9 | Western blotting

Western blotting was performed as described previously.[20] Anti-POLH (28133-1-AP, PGI, 1:1000) and anti-GAPDH (#2118, Cell Signaling Technology, 1:1000) were used as the primary antibodies. Anti-mouse IgG horseradish peroxidase (HRP)-linked antibody (#7076, Cell Signaling Technology, 1:2000) and anti-rabbit IgG HRP-linked antibody (#7074, Cell Signaling Technology, 1:2000) were used as the secondary antibodies.

2.10 | Dual-luciferase reporter assay

The POLH-3′-UTR fragment was amplified by PCR with primers from Table S6 and ligated into the XbaI and XhoI site of the pmirGLO luciferase reporter vector (Promega). For the reporter assay, the luciferase construct (100 ng) was cotransfected into the cells using Lipofectamine 3000 (Thermo Fisher Scientific) with 100 nmol/L CTRL ASO, 100 nmol/L TUG1 ASO, 50 nmol/L miRNA inhibitor, or 50 nmol/L miRNA inhibitor negative control. Luciferase activity was measured 48 h after transfection using a dual-luciferase reporter assay system (Promega). The relative luciferase activity was determined by normalizing firefly luminescence to Renilla luminescence.

2.11 | Immunohistochemistry (IHC)

Staining was performed on 5-μm sections of the OVCA tissues collected from patients ($n=72$). After de-paraffinization, antigen retrieval was performed in a microwave oven in 10 mM sodium citrate buffer (pH 6.0). Following a 3% H_2O_2 block for 20 min, specimens were incubated with the anti-POLH antibodies (HPA006721, 1:400, Sigma Aldrich). After subsequent incubation with HRP-conjugated secondary antibody, specimens were subjected to DAB (Agilent Technologies) and hematoxylin staining. The POLH IHC score was calculated using the following equation: IHC score$=\Sigma\ P_i\ (i)$, where i=intensity of

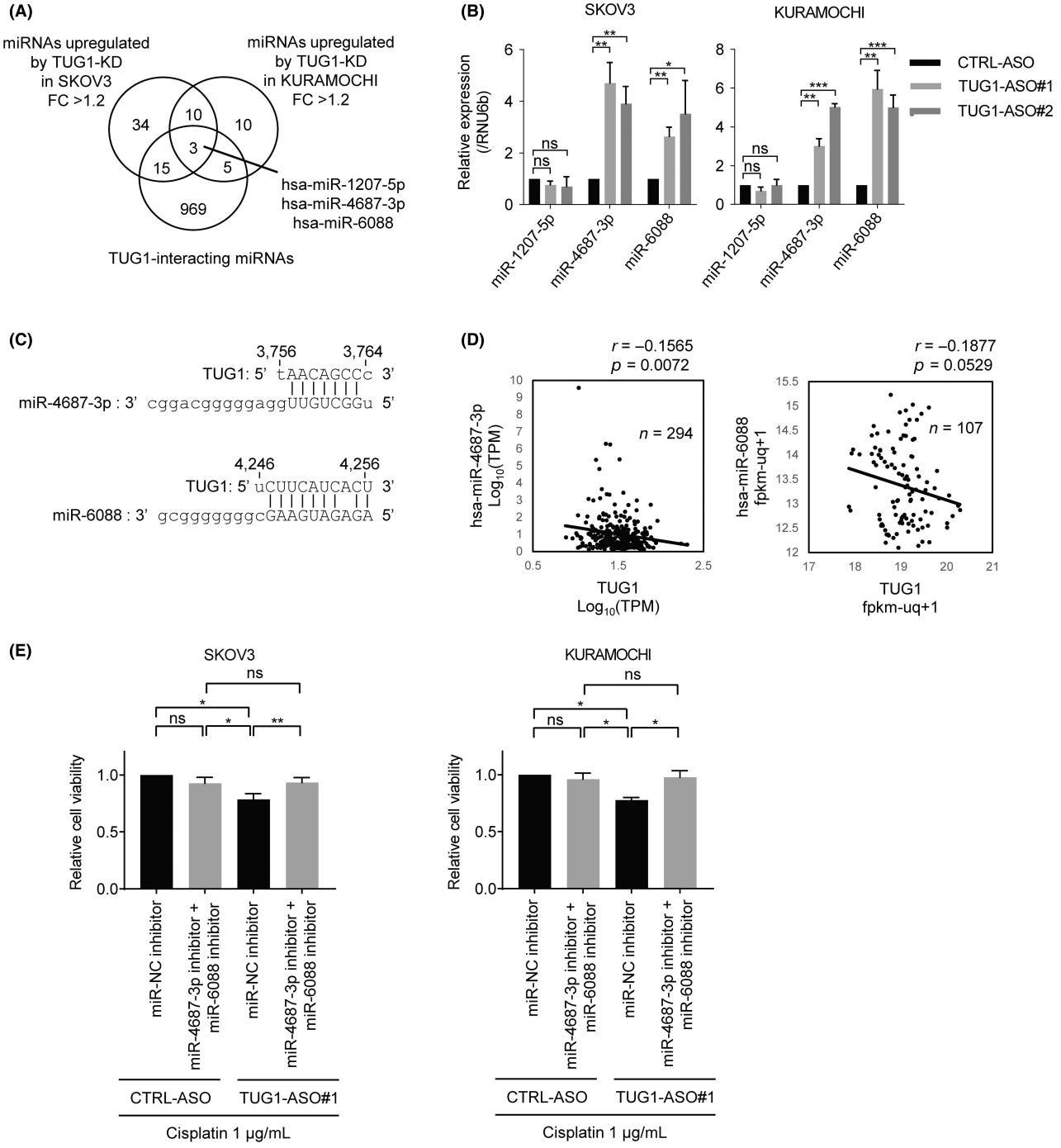

FIGURE 2 Taurine upregulated gene 1 (TUG1) promotes cisplatin resistance by downregulating miRNAs in ovarian cancer (OVCA) cell lines. (A) Venn diagram displaying miRNAs upregulated in SKOV3 and KURAMOCHI upon TUG1 depletion and those potentially binding to TUG1. FC, fold change. (B) qPCR analysis of miR-1207-5p, miR-4687-3p, and miR-6088 expression in SKOV3 and KURAMOCHI cells transfected with CTRL-ASO, TUG1-ASO#1, or TUG1-ASO#2 for 24 h. miRNA expression is normalized to RNU6b, and the *y*-axis shows relative expression compared with Ctrl ASO-treated cells. Data are mean ± SEM. $^{*}p < 0.05$; $^{**}p < 0.01$; $^{***}p < 0.001$, two-sided *t*-test, $n = 3$. (C) Predicted binding of miR-4687-3p and miR-6088 with TUG1. The seed sequence of miR-4687-3p and miR-6088, and the complementary sequence in TUG1 are depicted. (D) Scatter plots illustrating the Pearson correlation between TUG1 and miR-4687-3p expression (left, $n = 294$) and TUG1 and miR-6088 expression (right, $n = 107$) in OVCA samples from the TCGA database. The expression values in the former and later data were normalized to transformed reads per million (TPM) in the GDC Data Portal and fragments per kilobase million upper quantile +1 (fpkm-uq + 1) in the UCSC Xena, respectively. Pearson's correlation coefficients (*r*) with the corresponding *p*-values are shown. (E) Viability of SKOV3 and KURAMOCHI cells transfected with CTRL-ASO or TUG1-ASO#1 for 24 h, followed by incubation with 0.25 μg/mL cisplatin for 48 h. Cells were also transfected with miRNA inhibitor negative control (miR-NC inhibitor) or a combination of miR-4687-3p inhibitor and miR-6088 inhibitor along with CTRL-ASO or TUG1-ASO#1. The *y*-axis represents relative cell viability compared with Ctrl ASO- and miR-NC inhibitor-treated cells. Data are presented as mean ± SEM. $^{*}p < 0.05$; $^{**}p < 0.01$, two-sided *t*-test, $n = 3$.

staining (1, 2, or 3 as weak, moderate, or strong, respectively) and Pi is the percentage of stained cells for each intensity. The mean POLH IHC scores were obtained from a minimum of five fields in one section using an Olympus VS120 microscope (Olympus) at ×20 magnification.

2.12 | Construction of the POLH expression vector

The POLH gene was amplified by PCR using KOD-plus-neo (TOYOBO). The primer sequences are shown in Table S6. The amplified DNA fragment was cloned into pcDNA3.1(+) vector (Thermo Fisher Scientific) and validated by conventional sequencing analysis. Transfection of DNA vectors was performed using Lipofectamine 3000 according to the manufacturer's instructions (Thermo Fisher Scientific).

2.13 | Xenograft mouse model and treatment

SKOV3-Luc cells (2×10^6 per mouse) were intraperitoneally inoculated into 6-week-old female BALB/c nude mice (The Jackson Laboratory Japan). A cyclic Arg-Gly-Asp (cRGD) peptide-conjugated polymeric micelle was used as the drug delivery system (DDS) of TUG1 ASO in vivo.[20,22,30,31] The sequence used for the ASO was as follows: TUG1 ASO1: 5′-TGAATTTCAATCATTTGAGAT -3′. One week after the inoculation, TUG1-DDS (1 mg/kg of TUG1 ASO1 per day) was intraperitoneally injected every 3 days for three cycles and cisplatin (2.5 mg/kg per day) was intraperitoneally injected every 3 days for six cycles (started from nontreatment [$n=12$], cisplatin [$n=9$], TUG1-DDS [$n=9$], cisplatin and TUG1-DDS [$n=9$]). The bioluminescent imaging was conducted using an in vivo imaging system (IVIS, Xenogen Corp./Caliper Life Science) 1, 4, and 8 weeks after implantation. A 150-mg/kg dose of D-Luciferin potassium salt (Perkin-Elmer) was injected intraperitoneally into the mice 10 min before imaging. The mice were anesthetized using isoflurane and imaged dorsally. The region of interest (ROI) was selected, and the radiance value was measured by Living Image® 4.3.1 Software (Caliper Life Science). After treatment, tumors were harvested and profiled using Western blotting.

2.14 | Statistical analysis

Results are shown as mean, and the error bars represent the standard error of the mean (SE). The number of times experiments were repeated with similar results and the number (n) from which statistics are calculated are provided in the figure legend for each experiment. GraphPad Prism8 was used to generate graphs and to perform statistical analysis. p-Values were calculated using two-sided Student's t-tests unless stated otherwise. p-Values of statistical significance are indicated as ns, $p>0.05$, $^*p<0.05$, $^{**}p<0.01$, and $^{***}p<0.001$.

2.15 | Data resources

The microarray data and analyzed DRIP-seq data have been deposited in the Genomic Expression Archive (GEA) under accession code E-GEAD-602. The human cancer data from the TCGA were derived from the GDC Data Portal and UCSC Xena. The data of small-RNA sequencing in BEAS-2B cells (SRX463338)[32] were derived from miRmine[33] (https://guanfiles.dcmb.med.umich.edu/mirmine/index.html). All other data supporting the findings of this study are available from the corresponding authors upon reasonable request.

3 | RESULTS

3.1 | Expression status of TUG1 in OVCA patients treated with platinum-based chemotherapy

RNA-FISH analysis in 20 primary OVCAs revealed that the number of TUG1 spots in cancer cells is significantly upregulated cisplatin-resistant compared with cisplatin-sensitive patients ($n=9$ and 11,

FIGURE 3 Taurine upregulated gene 1 (TUG1) upregulates DNA polymerase eta (POLH) by inhibiting miR-4687-3p and miR-6088. (A) Venn diagram illustrating the common target genes of miR-4687-3p and miR-6088. Twenty genes are targeted by both miRNAs. (B) Predicted binding of miR-4687-3p (top) and miR-6088 (bottom) to POLH-mRNA 3′UTR. Seed sequences of miR-4687-3p and miR-6088, along with the complementary sequences in POLH 3′UTR, are shown. (C) Top: Representative Western blot images of SKOV3 and KURAMOCHI cells transfected with CTRL-ASO, TUG1-ASO#1, and TUG1-ASO#2 for 48 h. Anti-POLH and anti-GAPDH antibodies were used. Bottom: Bar graphs represent quantified Western blot data. Signal intensities are normalized to GAPDH, with values relative to CTRL-ASO, presented as mean ± SEM. $^*p<0.05$; $^{**}p<0.01$; $^{***}p<0.001$, two-sided t-test, $n=3$. (D) RT-qPCR analysis of POLH expression in SKOV3 and KURAMOCHI cells transfected with CTRL-ASO, TUG1-ASO#1, and TUG1-ASO#2 for 48 h. TUG1 expression is normalized to GAPDH and presented as mean ± SEM. $^*p<0.05$; $^{**}p<0.01$; $^{***}p<0.001$, two-sided t-test, $n=3$. (E) Top: Representative Western blot images of SKOV3 and KURAMOCHI cells transfected with TUG1-ASO#1 and miR-NC inhibitor, miR-4687-3p inhibitor, or miR-6088 inhibitor for 48 h. Anti-POLH and anti-GAPDH antibodies were used. Bottom: Bar graphs represent quantified Western blot data. Signal intensities are normalized to GAPDH, with values relative to the miR-NC inhibitor, presented as mean ± SEM. $^*p<0.05$; $^{**}p<0.01$, two-sided t-test, $n=3$. (F) Top: Representative Western blot images of SKOV3 and KURAMOCHI cells transfected with miR-NC mimic, miR-4687-3p mimic, or miR-6088 mimic together with CTRL-ASO for 48 h. Anti-POLH and anti-GAPDH antibodies were used. Bottom: Bar graphs represent quantified Western blot data. Signal intensities are normalized to GAPDH, with values relative to the miR-NC mimic, presented as mean ± SEM. $^*p<0.05$, two-sided t-test, $n=3$. (G) Dual-luciferase reporter assay in SKOV3 cells. The POLH 3'UTR reporter was cotransfected with miR-NC inhibitor, miR-4687 inhibitor, or miR-6088 inhibitor for 48 h. Cells were simultaneously transfected with CTRL-ASO or TUG1-ASO#1. Values are relative to the miR-NC inhibitor, presented as mean ± SEM. $^*p<0.05$, two-sided t-test, $n=3$.

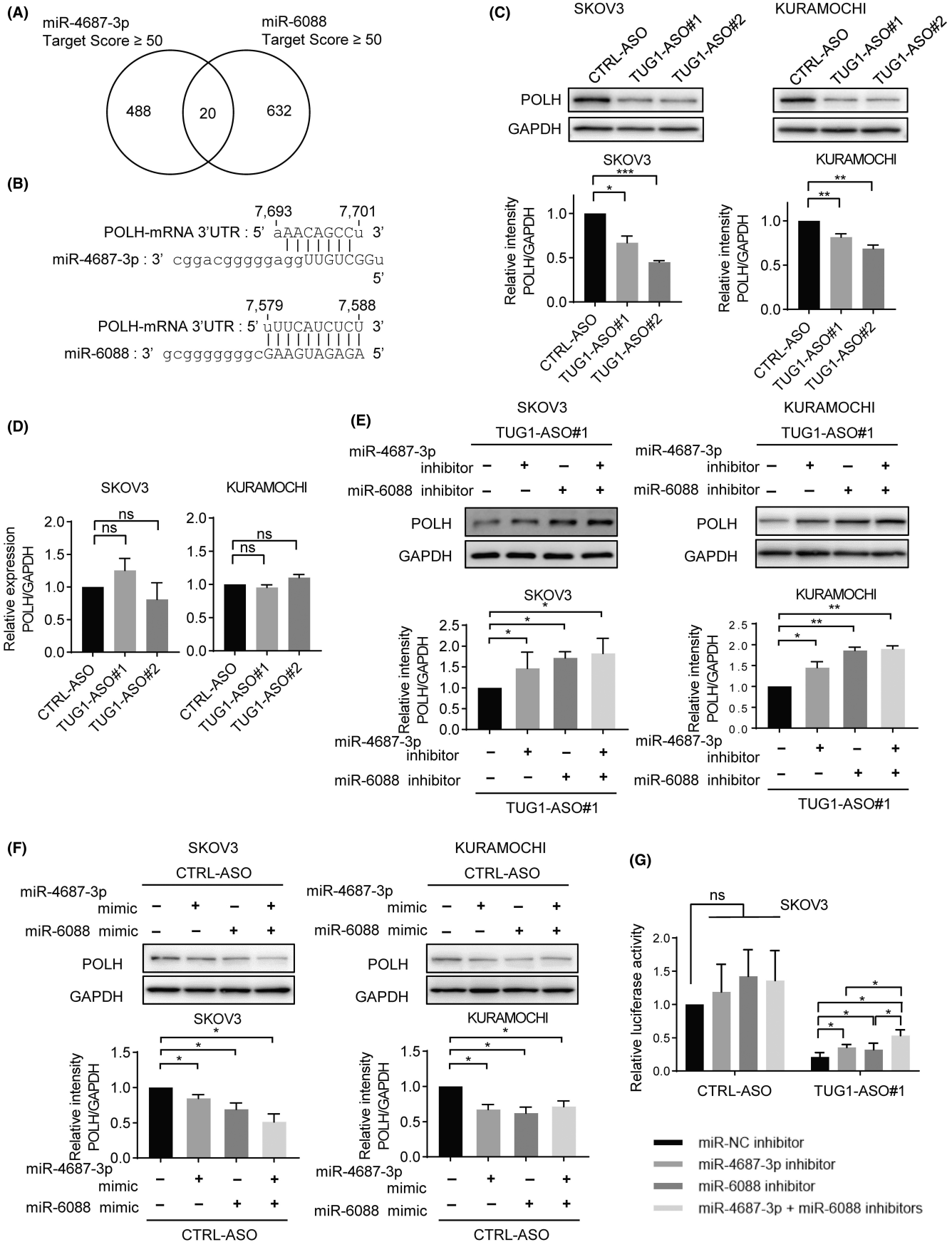
(A)
miR-4687-3p
Target Score ≥ 50
miR-6088
Target Score ≥ 50
488
20
632
(B)
7,693
7,701
POLH-mRNA 3'UTR : 5' aAACAGCCu 3'
miR-4687-3p : 3' cggacgggggaggUUGUCGGu 5'
7,579
7,588
POLH-mRNA 3'UTR : 5' uUUCAUCUCU 3'
miR-6088 : 3' gcgggggggcGAAGUAGAGA 5'
(C)
SKOV3
KURAMOCHI
CTRL-ASO
TUG1-ASO#1
TUG1-ASO#2
POLH
GAPDH
Relative intensity POLH/GAPDH
(D)
Relative expression POLH/GAPDH
ns
(E)
TUG1-ASO#1
miR-4687-3p inhibitor
miR-6088 inhibitor
(F)
CTRL-ASO
miR-4687-3p mimic
miR-6088 mimic
(G)
Relative luciferase activity
miR-NC inhibitor
miR-4687-3p inhibitor
miR-6088 inhibitor
miR-4687-3p + miR-6088 inhibitors

respectively; $p<0.01$, Figure 1A,B, Table S1). Specifically, TUG1 was upregulated approximately twofold in the cytoplasm of resistant cancers compared with that of sensitive cancers ($p<0.001$), while the number of nuclear TUG1 spots was similar between the two (Figure 1B). The levels of TUG1 expression were not different between early stages (I and II) and advanced stages (III and IV) (Figure 1B).

In TCGA dataset, 142 patients with primary OVCAs who underwent cisplatin-based chemotherapy were classified into two groups: the TUG1-high group ($n=69$, Z-score >0) and the TUG1-low group ($n=73$, Z-score <0) (Table S2). Relapse-free survival in the TUG1-high group was significantly shorter than that in the TUG1-low group ($p=0.0397$, log-rank test; HR = 0.662; 95% CI, 0.44–0.99; Figure 1C) suggesting that upregulation of TUG1 is related to poor prognosis in patients with OVCA who underwent cisplatin treatment.

3.2 | TUG1 depletion restores cisplatin sensitivity in cisplatin-resistant cells

We next examined the cytotoxic effects of cisplatin on multiple OVCA cell lines. Among 11 OVCA cell lines (Table S3), low TUG1 expression was observed in OVCA cell lines, ES2, EMGII, OVTOKO, and CAOV3. On the other hand, high TUG1 expression was found in JHOS2, OVCAR3, and SKOV3, with the highest expression observed in the KURAMOCHI cell line (Figure 1D). Therefore, we selected ES2 as a low-TUG1 cell line and KURAMOCHI and SKOV3 as high-TUG1 cell lines for follow-up studies. Interestingly, ES2 were more sensitive to cisplatin than SKOV3 and KURAMOCHI, which were relatively resistant, with IC50 values of 1.42 μg/mL for ES2, 2.89 μg/mL for SKOV3, and 2.35 μg/mL for KURAMOCHI (Figure 1E).

Depletion of TUG1 by two different specific ASO against TUG1 (TUG1-ASO#1 and #2; see[20] Figure 1F and Table S6) increased the sensitivity of both SKOV3 and KURAMOCHI to cisplatin (SKOV3 IC50: 2.89 μg/mL with CTRL-ASO decreased to 1.33 μg/mL and 1.01 μg/mL with TUG1-ASO#1 and TUG1-ASO#2, respectively, and KURAMOCHI IC50: 2.35 μg/mL with CTRL-ASO decreased to 1.29 μg/mL and 0.93 μg/mL with TUG1-ASO#1 and TUG1-ASO#2, respectively; Figure 1E). In contrast, depletion of TUG1 had less effect in ES2 cells (IC50: 1.42 μg/mL) with CTRL-ASO decreased to 1.06 μg/mL and 0.91 μg/mL with TUG1-ASO#1 and TUG1-ASO#2, respectively (Figure 1E). Overexpression of TUG1 in ES2 cells increased cisplatin resistance, with the IC50 rising from 1.40 μg/mL in the vector control to 2.12 μg/mL in cells transfected with pPGK-TUG1 (Figure 1G). The combination index[34] revealed that TUG1 depletion synergistically enhanced the cytotoxic effects of cisplatin in SKOV3 and KURAMOCHI (combination index of 2.5 μg/mL cisplatin and 100 μM TUG1-ASO#1, 0.27 and 0.29, respectively; Figure 1H).

3.3 | TUG1 promotes cisplatin resistance via downregulating miRNAs in OVCA cells

The significant increase in TUG1 expression in the cytoplasm of cisplatin-resistant clinical specimens suggests that TUG1 may exert its protective role in the cytoplasm, possibly through interactions with specific miRNAs.[10,35] We performed miRNA microarray analysis to investigate the impact of TUG1 depletion on miRNA expression. After treating SKOV3 and KURAMOCHI cells with TUG1-ASO#1, we observed the upregulation of 62 and 28 miRNAs more than 1.2-fold, respectively. (Figure 2A, Table S4). Among the 13 miRNAs that were commonly upregulated in both SKOV3 and KURAMOCHI cell lines, three of them (hsa-miR-1207-5p, hsa-miR-4687-3p, hsa-miR-6088) were predicted to interact with TUG1 based on in silico analysis using DIANA-LncBase (https://diana.e-ce.uth.gr/lncbasev3/home)[36] (Figure 2A). Upregulation of hsa-miR-4687-3p and hsa-miR-6088 after TUG1 depletion was further validated by qPCR analyses (Figure 2B). Indeed, the TUG1 sequence contains seven nucleotides that match the seed sequence of miR-4687-3p, and nine nucleotides that match the seed sequence of miR-6088. These matches suggest a potential interaction between TUG1 and these miRNAs (Figure 2C).

Correlation coefficient analysis revealed significant negative relationships between TUG1 and miR-4687-3p, as well as a trend of negative relationships between TUG1 and miR-6088 expression in OVCAs in TCGA dataset ($r=-0.16$, $p=0.0072$; $r=-0.19$, $p=0.053$, respectively; Figure 2D, Table S2). The level of miR-4687-3p and miR-6088 expression was lower in a normal fibroblast cell line, BEAS-2B, compared with OVCAs ($\mathrm{Log}_{10}(\mathrm{TPM})=0.23$ for hsa-miR-4687-3p and fpkm-uq + 1 = 1 for hsa-miR-6088).

Blockade of miR-4687-3p and miR-6088 using their respective miRNA inhibitors attenuated the toxicity of the cisplatin/TUG1-ASO

FIGURE 4 DNA polymerase eta (POLH) mediates taurine upregulated gene 1 (TUG1)-induced cisplatin resistance in ovarian cancer (OVCA). (A) Top: Dose–response curve of cisplatin in SKOV3 (left) and KURAMOCHI cells (right) transfected with siCTRL, siPOLH#1, or siPOLH#2 for 48 h, followed by incubation with cisplatin for 48 h. IC50 values for the indicated treatments are shown. Results are mean ± SEM, $n=3$. Bottom: Representative Western blot images of SKOV3 and KURAMOCHI cells transfected with siCTRL, siPOLH#1, or siPOLH#2 for 48 h. Anti-POLH and anti-GAPDH antibodies were used. (B) Left: Immunohistochemical analysis of POLH in cisplatin-sensitive and -resistant OVCA clinical samples. Scale bar: 30 μm. Right: Bar graph displaying POLH immunohistochemistry (IHC) scores for immunohistochemical analysis (sensitive, $n=63$; resistant, $n=9$) in OVCA clinical samples. $^{***}p<0.001$, two-sided Mann–Whitney U test. (C) Scatter plot illustrating the Pearson correlation between POLH H-scores from immunohistochemical analysis and the number of TUG1 spots per cell in RNA-FISH analysis in OVCA clinical samples. Data from cisplatin-sensitive clinical samples ($n=11$) and -resistant samples ($n=5$) are shown. Pearson's correlation determination R^2, with the corresponding p-value, is indicated. (D) Top: Dose–response curve of cisplatin in SKOV3 (left) and KURAMOCHI (right) cells transfected with CTRL-ASO, POLH-expressing vector (POLH OE), and TUG1-ASO#1 for 48 h, followed by incubation with cisplatin for 48 h. The IC50 value for the indicated treatment is shown. Results are mean ± SEM, $n=3$. Bottom: Representative Western blot images of SKOV3 and KURAMOCHI cells transfected with CTRL-ASO, POLH-expressing vector (POLH OE), and TUG1-ASO#1 for 48 h. Anti-POLH and anti-GAPDH antibodies were used.

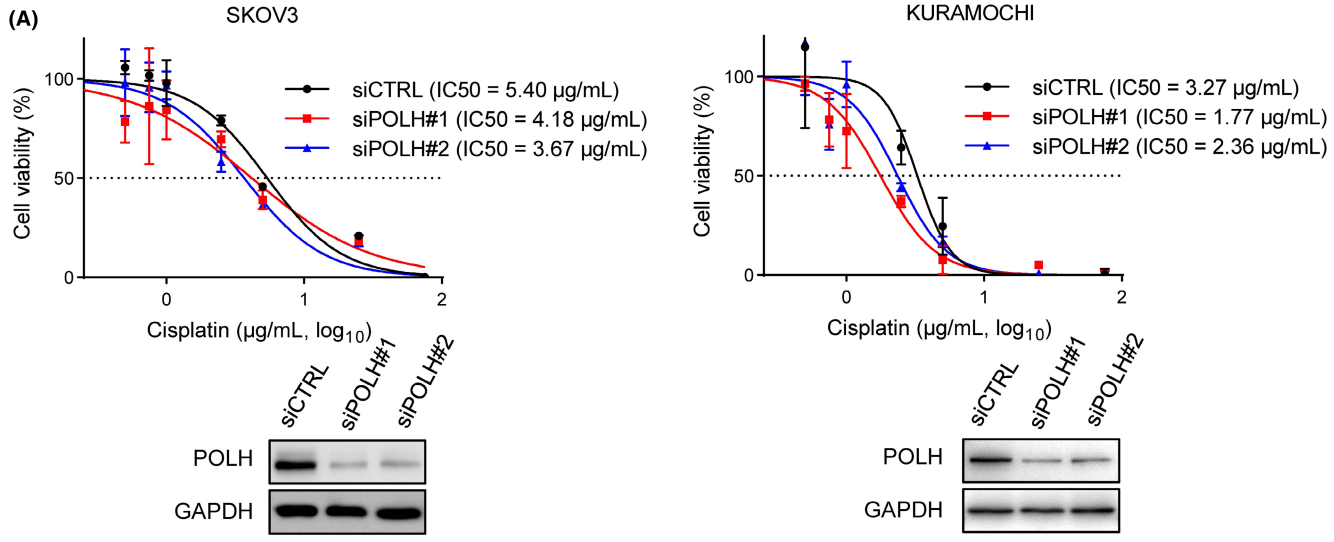
(A)
SKOV3
Cell viability (%)
siCTRL (IC50 = 5.40 μg/mL)
siPOLH#1 (IC50 = 4.18 μg/mL)
siPOLH#2 (IC50 = 3.67 μg/mL)
Cisplatin (μg/mL, log10)
siCTRL
siPOLH#1
siPOLH#2
POLH
GAPDH
KURAMOCHI
siCTRL (IC50 = 3.27 μg/mL)
siPOLH#1 (IC50 = 1.77 μg/mL)
siPOLH#2 (IC50 = 2.36 μg/mL)

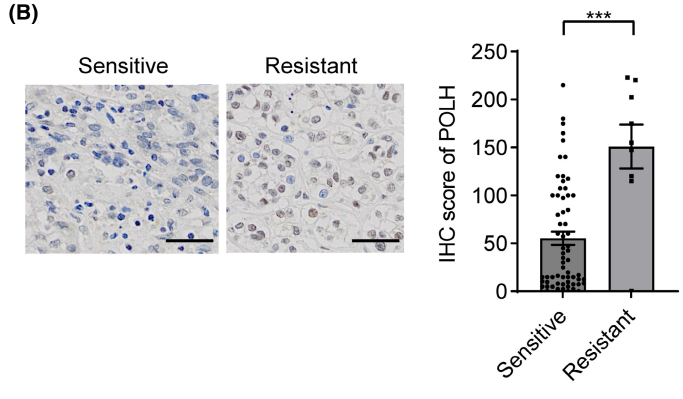
(B)
Sensitive
Resistant
IHC score of POLH
***
Sensitive
Resistant

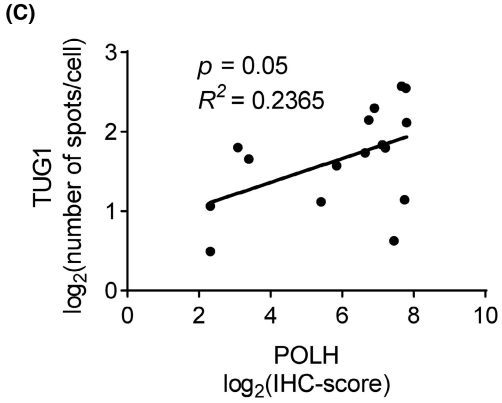
(C)
p = 0.05
R2 = 0.2365
TUG1
log2(number of spots/cell)
POLH
log2(IHC-score)

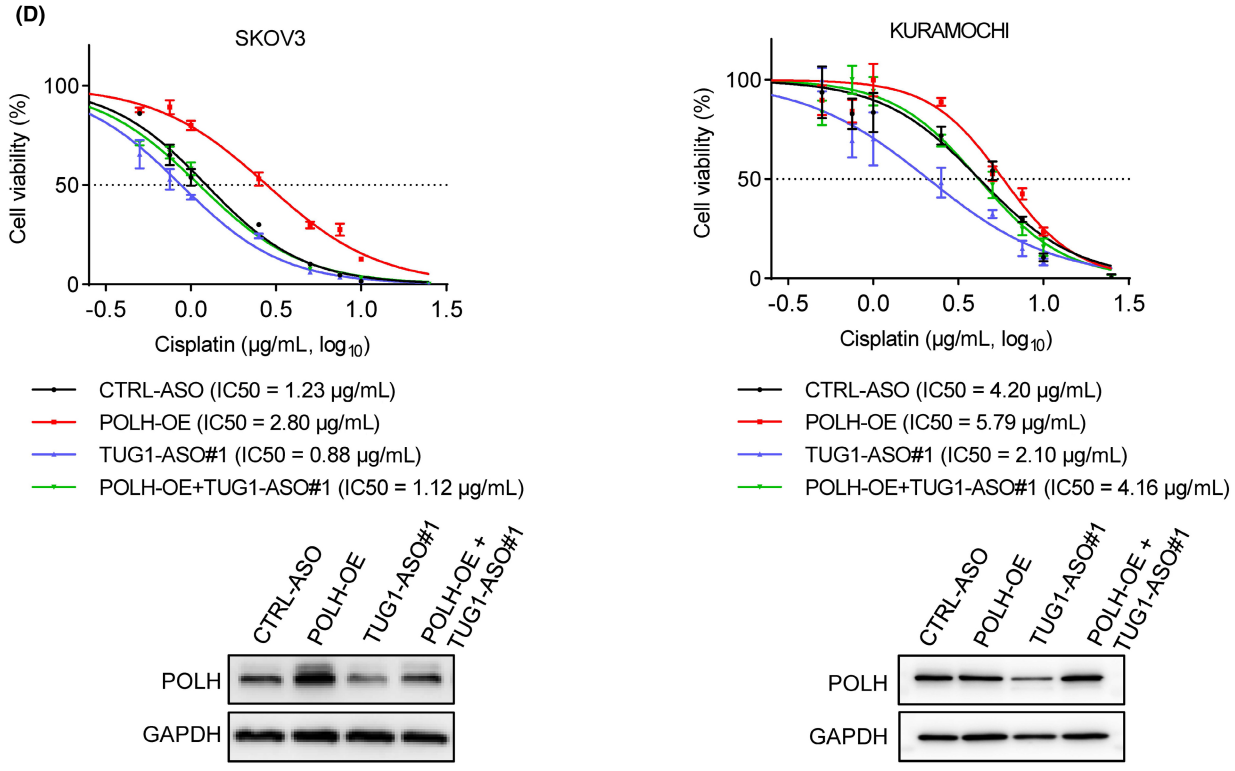
(D)
SKOV3
Cell viability (%)
Cisplatin (μg/mL, log10)
CTRL-ASO (IC50 = 1.23 μg/mL)
POLH-OE (IC50 = 2.80 μg/mL)
TUG1-ASO#1 (IC50 = 0.88 μg/mL)
POLH-OE+TUG1-ASO#1 (IC50 = 1.12 μg/mL)
CTRL-ASO
POLH-OE
TUG1-ASO#1
POLH-OE + TUG1-ASO#1
POLH
GAPDH
KURAMOCHI
CTRL-ASO (IC50 = 4.20 μg/mL)
POLH-OE (IC50 = 5.79 μg/mL)
TUG1-ASO#1 (IC50 = 2.10 μg/mL)
POLH-OE+TUG1-ASO#1 (IC50 = 4.16 μg/mL)

combination treatment in SKOV3 and KURAMOCHI cells (Figure 2E). These results indicate that the repression of miR-4687-3p and miR-6088 by TUG1 is associated with the development of cisplatin resistance in OVCA cells.

3.4 | POLH is a downstream target of miRNAs that bind TUG1

To identify target genes linked to the acquisition of cisplatin resistance regulated by miR-4687-3p and miR-6088, we conducted in silico analysis using the miRDB database (https://mirdb.org/).[37] We examined the function of 20 genes that were identified as common potential targets of both miR-4687-3p and miR-6088 (Figure 3A, Table S5). Among these, POLH was selected for further analysis due to its significant role in TLS and its established connection with the DNA damage response and DNA repair,[26–28] both processes that can modulate the mechanistic effects of cisplatin.

The seed sequences of the miR-4687-3p and miR-6088 binding regions in the 3'-UTR of *POLH* mRNA are depicted in Figure 3B. Notably, depletion of TUG1 significantly suppressed POLH protein expression in both SKOV3 and KURAMOCHI cells (Figure 3C). Interestingly, the mRNA expression level remained largely unchanged or even exhibited a slight increase (Figure 3D). These findings suggest that the substantial downregulation of POLH caused by TUG1 depletion occurs primarily at the translational level, with little to no impact on mRNA decay mediated by miRNAs.[38] Consistently, inhibition of the miRNAs upregulated POLH protein expression under TUG1-depleted conditions (Figure 3E), whereas miRNA overexpression reduced POLH protein expression in both SKOV3 and KURAMOCHI cells (Figure 3F).

The functional interaction between TUG1, miR-4687-3p and miR-6088, and 3'-UTR of *POLH* was examined using dual-luciferase reporter assays. TUG1 depletion significantly decreased luciferase activity (Figure 3G). Furthermore, blockade of miR-4687-3p and miR-6088 using miRNA inhibitors significantly upregulated luciferase activity when TUG1 was depleted but had no effect in the CTRL-ASO treated cells. The combined inhibition of miR-4687-3p and miR-6088 yielded the strongest reversal of the effect of TUG1 depletion (Figure 3G).

3.5 | POLH mediates TUG1-dependent cisplatin resistance in OVCA

Depletion of POLH using siRNA lowered the IC50 for cisplatin in both SKOV3 and KURAMOCHI cells (Figure 4A). In clinical samples, POLH expression was higher in cisplatin-resistant OVCA cases compared with -sensitive ones (Figure 4B). Moreover, smFISH revealed a trend of positive correlation between POLH expression and TUG1 expression in OVCA clinical samples ($n=16$, $R^2=0.24$, $p=0.05$) (Figure 4C). Finally, overexpression of POLH reversed the effects of TUG1 depletion (Figure 4D). Collectively, these findings suggest that the TUG1-POLH axis plays a key role in cisplatin resistance in OVCA.

3.6 | Targeting TUG1 sensitizes OVCA cells to cisplatin in vivo

Next, we examined the impact of combination therapy with cisplatin and TUG1-ASO in an OVCA xenograft mouse model in vivo. To achieve an effective in vivo ASO delivery, we employed a cRGD peptide-conjugated polymeric micelle DDS, termed TUG1-DDS, as previously described.[20,30,31,39] Mice bearing SKOV3 xenograft tumors were subjected to intraperitoneal treatment with TUG1-DDS (administered every 3 days for three cycles) and/or cisplatin (given every 3 days for six cycles) (Figure 5A). TUG1-DDS effectively accumulated within the xenograft tumors, significantly suppressing their growth compared with the nontreated group (Figure 5B). Notably, by 8 weeks post xenograft injection, the combination of both cisplatin and TUG1-DDS exhibited a more substantial inhibition of tumor growth than TUG1-DDS alone (Figure 5B). Consistent with our in vitro findings, POLH expression was lower in tumors treated with TUG1-DDS (Figure 5C).

4 | DISCUSSION

In the current study, we have demonstrated that targeting the TUG1-miR-4687-3p/miR-6088-POLH axis enhances cisplatin sensitivity, specifically in OVCA cases characterized by high TUG1 expression (Figure 5D). Due to its inhibition of miRNAs, the lncRNA TUG1 is reported as a promoter of cisplatin resistance and cancer progression

FIGURE 5 Tumor growth suppression by combination therapy with cisplatin and taurine upregulated gene 1 drug delivery system (TUG1-DDS). (A) Schematic depicting of the treatment protocol for xenograft mouse models. SKOV3-Luc cells were intraperitoneally injected into BALB/c nude mice (black arrow). Mice were treated with TUG1-DDS and/or cisplatin during the periods indicated by double-headed arrows. Bioluminescence signals were acquired at 1, 4, and 8 weeks post inoculation using the IVIS system (red arrowheads) (B) Top: Representative images of bioluminescence signals in mice for each treatment. Bottom: Quantification of bioluminescence signals in xenograft mouse models. The initial numbers of mice examined for each of the four experimental groups are indicated: non-treatment ($n=12$), cisplatin ($n=9$), TUG1-DDS ($n=9$), and cisplatin and TUG1-DDS ($n=9$). Results are mean ± SEM. $^{*}p<0.05$, two-way ANOVA with Bonferroni post hoc test. (C) Top: Western blot image of tumors obtained from the mouse xenografts. Anti-POLH and anti-GAPDH antibodies were used. Bottom: Bar graph displaying quantified Western blot data. Signal intensities were normalized to GAPDH, with values relative to CTRL-DDS and presented as mean ± SEM, $n=3$. $^{**}p<0.001$, two-sided *t*-test. (D) Conceptual diagram depicting TUG1-dependent cisplatin resistance in ovarian cancers (OVCAs). The heightened expression of TUG1 contributes to a reduction in the levels of miR-4687-3p and miR-6088. This decrease subsequently triggers the translational upregulation of POLH, which engenders cisplatin resistance (left). TUG1-targeted interventions may provide a therapeutic strategy to address cisplatin resistance in OVCAs (right).

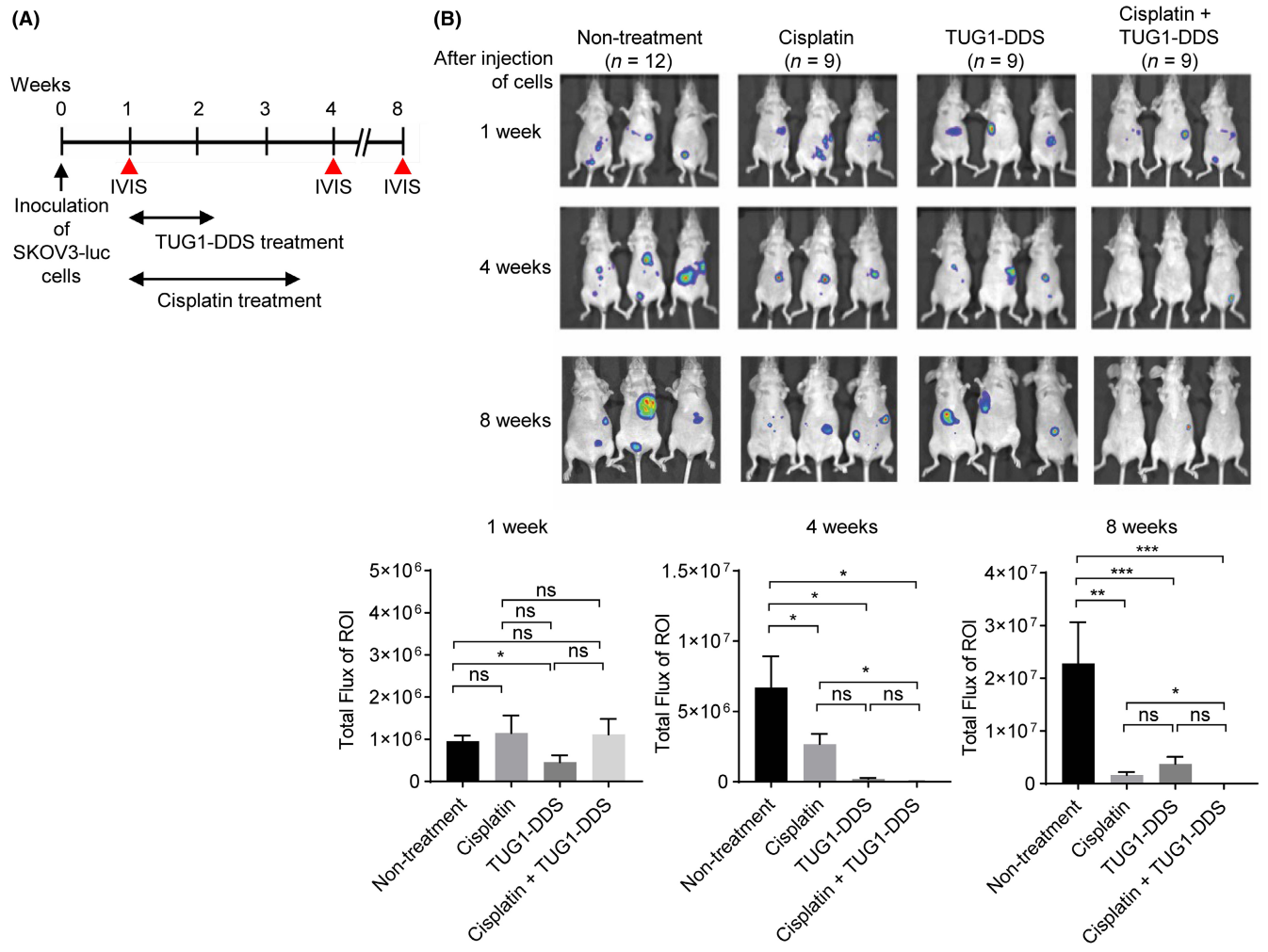

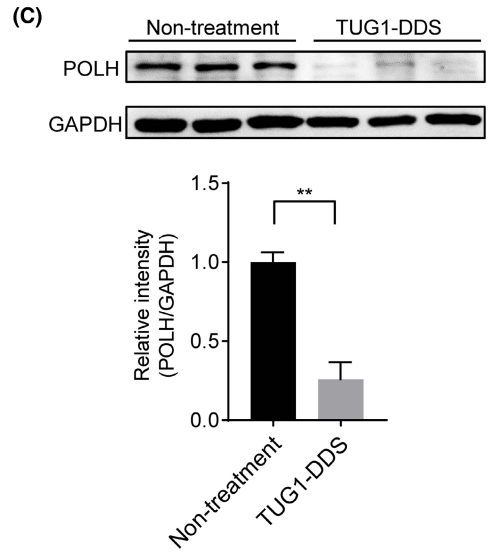

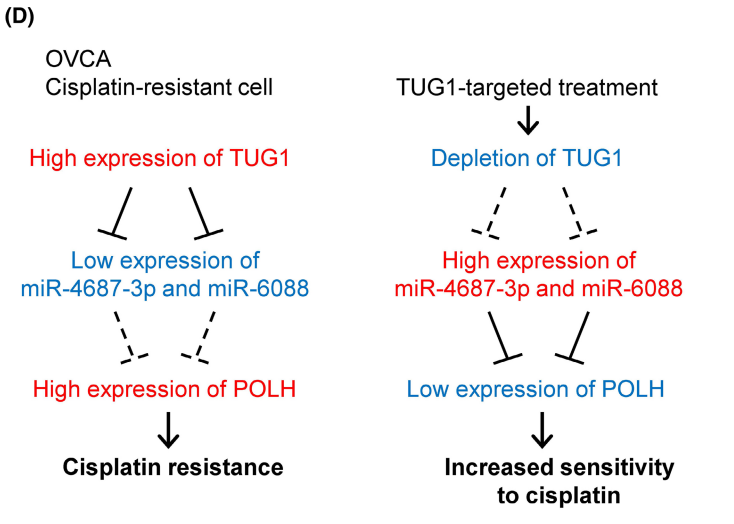

in various malignancies, including OVCA.[40–43] By contrast, TUG1 can also sensitize non-small cell lung cancer and triple-negative breast cancer.[44,45] In this study, we demonstrated that high expression of TUG1 in OVCA confers intrinsic resistance to cisplatin. Mechanistically, TUG1 upregulates POLH by acting as a competing endogenous RNA (ceRNA) for miR-4687-3p and miR-6088. Our findings, and those of others clearly show that TUG1 plays a pivotal role in regulating chemosensitivity in a context-dependent manner by interacting with tumor-specific miRNAs. The presence of ceRNAs creates competition between transcripts with shared miRNA binding sites, which can shape gene expression profiles.[38] Although the precise mechanisms by which this competition occurs remains unclear, there is now a

substantial amount of empirical evidence supporting the ceRNA competition hypothesis; this includes our previous studies on TUG1.[20,22]

POLH is the product of the xeroderma pigmentosum variant (XPV) gene and a well-characterized Y-family DNA polymerase for translesion synthesis.[46] Previous studies revealed that suppression of POLH expression promoted cisplatin-induced apoptosis of cancer stem cells isolated from OVCA cell lines and primary tumors.[47] Through TLS, the cross-links added by cisplatin-based drugs are bypassed during replication.[48] POLH is also associated with cisplatin resistance in lung and bladder cancers.[49] In these studies, POLH was targeted by miR-93[47] and miR-619.[49] Our present findings suggest that cytoplasmic TUG1 serves as a novel regulator of POLH through the reduction of miRNAs, thereby playing a pivotal role in the development of acquired cisplatin resistance. We suggest that cells with elevated TUG1 expression become dominant after cisplatin treatment, which would be consistent with the upregulation of TUG1 in samples from cisplatin-resistant OVCA patients. Functional experiments showed that TUG1 depletion essentially liberates miR-4687-3p and miR-6088, allowing them to bind POLH mRNA and suppress translation, thereby enhancing sensitivity to cisplatin. In contrast to earlier studies, we did not identify miR-93 and miR-619 as miRNAs regulated by TUG1; this may be due to our use of different cancer types when compared with those previously studied.

Recently, we have reported the essential role of TUG1 in suppressing cancer-specific replication stress (RS).[50] Excessive RS leads to DNA damage that would be cytotoxic to normal cells, and TUG1 upregulation therefore acts as a cancer cell-specific buffer to prevent tumor cell death. Notably, this function is carried out by nuclear TUG1 and is distinct from the cytoplasmic role of TUG1 as a ceRNA that regulates POLH expression, as discovered in the current study. Thus, TUG1 is engaged in different interactions with distinct target molecules in the cytoplasm and nucleus, yet its activity converges on mechanisms associated with DNA damage repair and maintenance of genome stability. The multifaceted role of TUG1 underscores its significance as a potential therapeutic target for modulating genomic instability and chemosensitivity in cancer cells.

Arg-Gly-Asp peptides targeting αvβ3 and αvβ5 integrins have been proposed as a promising DDS in OVCA cells.[51] In the current study, TUG1-ASO coupled with a cancer-specific cRGD peptide-conjugated polymeric micelle DDS[20,30,31] was efficiently taken up by endocytosis and transcytosis-mediated penetration and robustly suppressed the growth of OVCA in vivo. Although further investigations are required, cRGD-mediated drug delivery may be a powerful strategy for targeting OVCA.

In conclusion, our data indicate that the combination of conventional cisplatin therapy with TUG1-DDS represents a novel therapeutic strategy for inhibiting the growth of cisplatin-resistant OVCA. This approach holds significant potential for improving overall survival outcomes in these patients.

AUTHOR CONTRIBUTIONS

Ryosuke Sonobe: Investigation; writing – original draft. **Peng Yang:** Investigation; writing – original draft. **Miho M. Suzuki:** Investigation; writing – original draft. **Keiko Shinjo:** Investigation; writing – review and editing. **Kenta Iijima:** Investigation; writing – review and editing. **Nobuhiro Nishiyama:** Resources; writing – review and editing. **Kanjiro Miyata:** Resources; writing – review and editing. **Kazunori Kataoka:** Resources; writing – review and editing. **Hiroaki Kajiyama:** Writing – review and editing. **Yutaka Kondo:** Conceptualization; supervision; writing – review and editing.

ACKNOWLEDGMENTS

We thank Dr. Zhao Meng for her technical assistance. This study was supported by the Japan Agency for Medical Research and Development (23ck0106816h0001, 23ama221204h0002, Y.K.) and performed as a research program of the Grant-in-Aid for Scientific Research, Japan Society for the Promotion of Science (23H02747, Y.K.).

CONFLICT OF INTEREST STATEMENT

Y.K. and N.N. are current editorial board members of *Cancer Science*. The other authors have no conflict of interest to declare.

ETHICS STATEMENT

Approval of the research protocol by an Institutional Reviewer Board: OVCA samples were collected in accordance with the guidelines established by the Ethics Committee of Nagoya University (approval number 2020-0570).

Informed Consent: N/A.

Registry and the Registration No. of the study/trial: N/A.

Animal Studies: Animal protocols were approved by the Animal Care and Use Committee of Nagoya University Graduate School of Medicine (approval number 20268).

ORCID

Ryosuke Sonobe https://orcid.org/0009-0003-5297-347X
Miho M. Suzuki https://orcid.org/0000-0002-8882-6610
Keiko Shinjo https://orcid.org/0000-0002-7797-6453
Kenta Iijima https://orcid.org/0009-0004-1996-8940
Nobuhiro Nishiyama https://orcid.org/0000-0002-6886-9357
Kanjiro Miyata https://orcid.org/0000-0001-7044-190X
Kazunori Kataoka https://orcid.org/0000-0002-8591-413X
Hiroaki Kajiyama https://orcid.org/0000-0003-0493-1825
Yutaka Kondo https://orcid.org/0000-0003-3746-3191

REFERENCES

1. Sung H, Ferlay J, Siegel RL, et al. Global cancer statistics 2020: GLOBOCAN estimates of incidence and mortality worldwide for 36 cancers in 185 countries. *CA Cancer J Clin*. 2021;71:209-249.
2. Torre LA, Trabert B, DeSantis CE, et al. Ovarian cancer statistics, 2018. *CA Cancer J Clin*. 2018;68:284-296.
3. Ushijima K. Treatment for recurrent ovarian cancer-at first relapse. *J Oncol*. 2010;2010:497429.
4. Bast RC Jr, Hennessy B, Mills GB. The biology of ovarian cancer: new opportunities for translation. *Nat Rev Cancer*. 2009;9:415-428.
5. Agarwal R, Kaye SB. Ovarian cancer: strategies for overcoming resistance to chemotherapy. *Nat Rev Cancer*. 2003;3:502-516.

6. Ortiz M, Wabel E, Mitchell K, Horibata S. Mechanisms of chemotherapy resistance in ovarian cancer. *Cancer Drug Resist*. 2022;5:304-316.
7. Lee JM, Minasian L, Kohn EC. New strategies in ovarian cancer treatment. *Cancer*. 2019;125(Suppl 24):4623-4629.
8. Kelland L. The resurgence of platinum-based cancer chemotherapy. *Nat Rev Cancer*. 2007;7:573-584.
9. Siddik ZH. Cisplatin: mode of cytotoxic action and molecular basis of resistance. *Oncogene*. 2003;22:7265-7279.
10. Peng Y, Tang D, Zhao M, Kajiyama H, Kikkawa F, Kondo Y. Long non-coding RNA: a recently accentuated molecule in chemoresistance in cancer. *Cancer Metastasis Rev*. 2020;39:825-835.
11. Zon A, Bednarek I. Cisplatin in ovarian cancer treatment-known limitations in therapy force new solutions. *Int J Mol Sci*. 2023;24:7585.
12. Damia G, Broggini M. Platinum resistance in ovarian cancer: role of DNA repair. *Cancers (Basel)*. 2019;11:119.
13. Rocha CRR, Silva MM, Quinet A, Cabral-Neto JB, Menck CFM. DNA repair pathways and cisplatin resistance: an intimate relationship. *Clinics (Sao Paulo)*. 2018;73:e478s.
14. Martin SA, Lord CJ, Ashworth A. Therapeutic targeting of the DNA mismatch repair pathway. *Clin Cancer Res*. 2010;16:5107-5113.
15. Zhang C, Gao S, Hou J. ERCC1 expression and platinum chemosensitivity in patients with ovarian cancer: a meta-analysis. *Int J Biol Markers*. 2020;35:12-19.
16. Darzynkiewicz Z, Traganos F, Wlodkowic D. Impaired DNA damage response–an Achilles' heel sensitizing cancer to chemotherapy and radiotherapy. *Eur J Pharmacol*. 2009;625:143-150.
17. Schmitt AM, Chang HY. Long noncoding RNAs in cancer pathways. *Cancer Cell*. 2016;29:452-463.
18. Deguchi S, Katsushima K, Hatanaka A, et al. Oncogenic effects of evolutionarily conserved noncoding RNA ECONEXIN on gliomagenesis. *Oncogene*. 2017;36:4629-4640.
19. Liu K, Gao L, Ma X, et al. Long non-coding RNAs regulate drug resistance in cancer. *Mol Cancer*. 2020;19:54.
20. Katsushima K, Natsume A, Ohka F, et al. Targeting the notch-regulated non-coding RNA TUG1 for glioma treatment. *Nat Commun*. 2016;7:13616.
21. Da M, Zhuang J, Zhou Y, Qi Q, Han S. Role of long noncoding RNA taurine-upregulated gene 1 in cancers. *Mol Med*. 2021;27:51.
22. Tasaki Y, Suzuki M, Katsushima K, et al. Cancer-specific targeting of taurine-upregulated gene 1 enhances the effects of chemotherapy in pancreatic cancer. *Cancer Res*. 2021;81:1654-1666.
23. Zhan FL, Chen CF, Yao MZ. LncRNA TUG1 facilitates proliferation, invasion and stemness of ovarian cancer cell via miR-186-5p/ZEB1 axis. *Cell Biochem Funct*. 2020;38:1069-1078.
24. Pei Y, Li K, Lou X, et al. [corrigendum] miR-1299/NOTCH3/TUG1 feedback loop contributes to the malignant proliferation of ovarian cancer. *Oncol Rep*. 2023;49:96.
25. Gu L, Li Q, Liu H, Lu X, Zhu M. Long noncoding RNA TUG1 promotes autophagy-associated paclitaxel resistance by sponging miR-29b-3p in ovarian cancer cells. *Onco Targets Ther*. 2020;13:2007-2019.
26. Masutani C, Kusumoto R, Iwai S, Hanaoka F. Mechanisms of accurate translesion synthesis by human DNA polymerase eta. *EMBO J*. 2000;19:3100-3109.
27. McCulloch SD, Kokoska RJ, Masutani C, Iwai S, Hanaoka F, Kunkel TA. Preferential cis-syn thymine dimer bypass by DNA polymerase eta occurs with biased fidelity. *Nature*. 2004;428:97-100.
28. Saha P, Mandal T, Talukdar AD, et al. DNA polymerase eta: a potential pharmacological target for cancer therapy. *J Cell Physiol*. 2021;236:4106-4120.
29. Balcells I, Cirera S, Busk PK. Specific and sensitive quantitative RT-PCR of miRNAs with DNA primers. *BMC Biotechnol*. 2011;11:70.
30. Miura Y, Takenaka T, Toh K, et al. Cyclic RGD-linked polymeric micelles for targeted delivery of platinum anticancer drugs to glioblastoma through the blood–brain tumor barrier. *ACS Nano*. 2013;7:8583-8592.
31. Miyano K, Cabral H, Miura Y, et al. cRGD peptide installation on cisplatin-loaded nanomedicines enhances efficacy against locally advanced head and neck squamous cell carcinoma bearing cancer stem-like cells. *J Control Release*. 2017;261:275-286.
32. Zhao W, Pollack JL, Blagev DP, Zaitlen N, McManus MT, Erle DJ. Massively parallel functional annotation of 3′ untranslated regions. *Nat Biotechnol*. 2014;32:387-391.
33. Panwar B, Omenn GS, Guan Y. miRmine: a database of human miRNA expression profiles. *Bioinformatics*. 2017;33:1554-1560.
34. Zhao L, Wientjes MG, Au JL. Evaluation of combination chemotherapy: integration of nonlinear regression, curve shift, isobologram, and combination index analyses. *Clin Cancer Res*. 2004;10:7994-8004.
35. Salmena L, Poliseno L, Tay Y, Kats L, Pandolfi PP. A ceRNA hypothesis: the Rosetta stone of a hidden RNA language? *Cell*. 2011;146:353-358.
36. Paraskevopoulou MD, Vlachos IS, Karagkouni D, et al. DIANA-LncBase v2: indexing microRNA targets on non-coding transcripts. *Nucleic Acids Res*. 2016;44:D231-D238.
37. Chen Y, Wang X. miRDB: an online database for prediction of functional microRNA targets. *Nucleic Acids Res*. 2020;48:D127-D131.
38. Filipowicz W, Bhattacharyya SN, Sonenberg N. Mechanisms of post-transcriptional regulation by microRNAs: are the answers in sight? *Nat Rev Genet*. 2008;9:102-114.
39. Nishida H, Matsumoto Y, Kawana K, et al. Systemic delivery of siRNA by actively targeted polyion complex micelles for silencing the E6 and E7 human papillomavirus oncogenes. *J Control Release*. 2016;231:29-37.
40. Long J, Menggen Q, Wuren Q, Shi Q, Pi X. Long noncoding RNA taurine-upregulated Gene1 (TUG1) promotes tumor growth and metastasis through TUG1/Mir-129-5p/astrocyte-elevated Gene-1 (AEG-1) Axis in malignant melanoma. *Med Sci Monit*. 2018;24:1547-1559.
41. Yu G, Zhou H, Yao W, Meng L, Lang B. lncRNA TUG1 promotes cisplatin resistance by regulating CCND2 via epigenetically silencing miR-194-5p in bladder cancer. *Mol Ther Nucleic Acids*. 2019;16:257-271.
42. Zhang Z, Xiong R, Li C, Xu M, Guo M. LncRNA TUG1 promotes cisplatin resistance in esophageal squamous cell carcinoma cells by regulating Nrf2. *Acta Biochim Biophys Sin*. 2019;51:826-833.
43. El-Khazragy N, Mohammed HF, Yassin M, et al. Tissue-based long non-coding RNAs "PVT1, TUG1 and MEG3" signature predicts cisplatin resistance in ovarian cancer. *Genomics*. 2020;112:4640-4646.
44. Guo S, Zhang L, Zhang Y, et al. Long non-coding RNA TUG1 enhances chemosensitivity in non-small cell lung cancer by impairing microRNA-221-dependent PTEN inhibition. *Aging (Albany NY)*. 2019;11:7553-7569.
45. Tang T, Cheng Y, She Q, et al. Long non-coding RNA TUG1 sponges miR-197 to enhance cisplatin sensitivity in triple negative breast cancer. *Biomed Pharmacother*. 2018;107:338-346.
46. Fleck O, Schar P. Translesion DNA synthesis: little fingers teach tolerance. *Curr Biol*. 2004;14:R389-R391.
47. Srivastava AK, Han C, Zhao R, et al. Enhanced expression of DNA polymerase eta contributes to cisplatin resistance of ovarian cancer stem cells. *Proc Natl Acad Sci U S A*. 2015;112:4411-4416.
48. Knobel PA, Marti TM. Translesion DNA synthesis in the context of cancer research. *Cancer Cell Int*. 2011;11:39.
49. Zhang J, Sun W, Ren C, Kong X, Yan W, Chen X. A PolH transcript with a short 3'UTR enhances PolH expression and mediates cisplatin resistance. *Cancer Res*. 2019;79:3714-3724.

50. Suzuki MM, Iijima K, Ogami K, et al. TUG1-mediated R-loop resolution at microsatellite loci as a prerequisite for cancer cell proliferation. *Nat Commun*. 2023;14:4521.
51. Kobayashi M, Sawada K, Kimura T. Potential of integrin inhibitors for treating ovarian cancer: a literature review. *Cancer*. 2017;9:9.

SUPPORTING INFORMATION

Additional supporting information can be found online in the Supporting Information section at the end of this article.

How to cite this article: Sonobe R, Yang P, Suzuki MM, et al. Long noncoding RNA *TUG1* promotes cisplatin resistance in ovarian cancer via upregulation of DNA polymerase eta. *Cancer Sci*. 2024;115:1910-1923. doi:10.1111/cas.16150